Supporting Information

Hexabenzocoronene@Laponite Ion Cage: a Secondary Nanoassembly as Efficient Elastic Ion Platform

*Wenhao Wang,[ab], Yongrui Li, [ab], Jiamin Cheng,[ab], Yao Wang, [ab], Jingxing Zhang, *[abc], Zhenyu Xing, *[d], Hao Li,*[ab], and Guofu Zhou[ab]*

[a] *Guangdong Provincial Key Laboratory of Optical Information Materials and Technology, Institute of Electronic Paper Displays, South China Academy of Advanced Optoelectronics, South China Normal University, Guangzhou 510006, P. R. China*

[b] *National Center for International Research on Green Optoelectronics, South China Normal University, Guangzhou 510006, P. R. China*

[c] *Faculty of Materials Science and Engineering/Institute of Technology for Carbon Neutrality, Shenzhen Institute of Advanced Technology, Chinese Academy of Sciences, Shenzhen, Guangdong, 518055, China*

[d] *School of Chemistry, South China Normal University, Guangzhou 510006, China*

* Corresponding should be addressed to:

Dr. Jingxing Zhang; Tel: +86-20-39314813; Fax: +86-20-39314813

E-mail: Zhangjingxing2022@163.com

Associate Professor Zhenyu Xing Tel: +86-20-39314813; Fax: +86-20-39314813

E-mail: xingzhenyu@m.scnu.edu.cn; orcid.org/0000-0003-1655-7893

Professor Hao Li; Tel: +86-20-39314813; Fax: +86-20-39314813

E-mail: haoli@scnu.edu.cn; orcid.org/0000-0003-1744-1526;

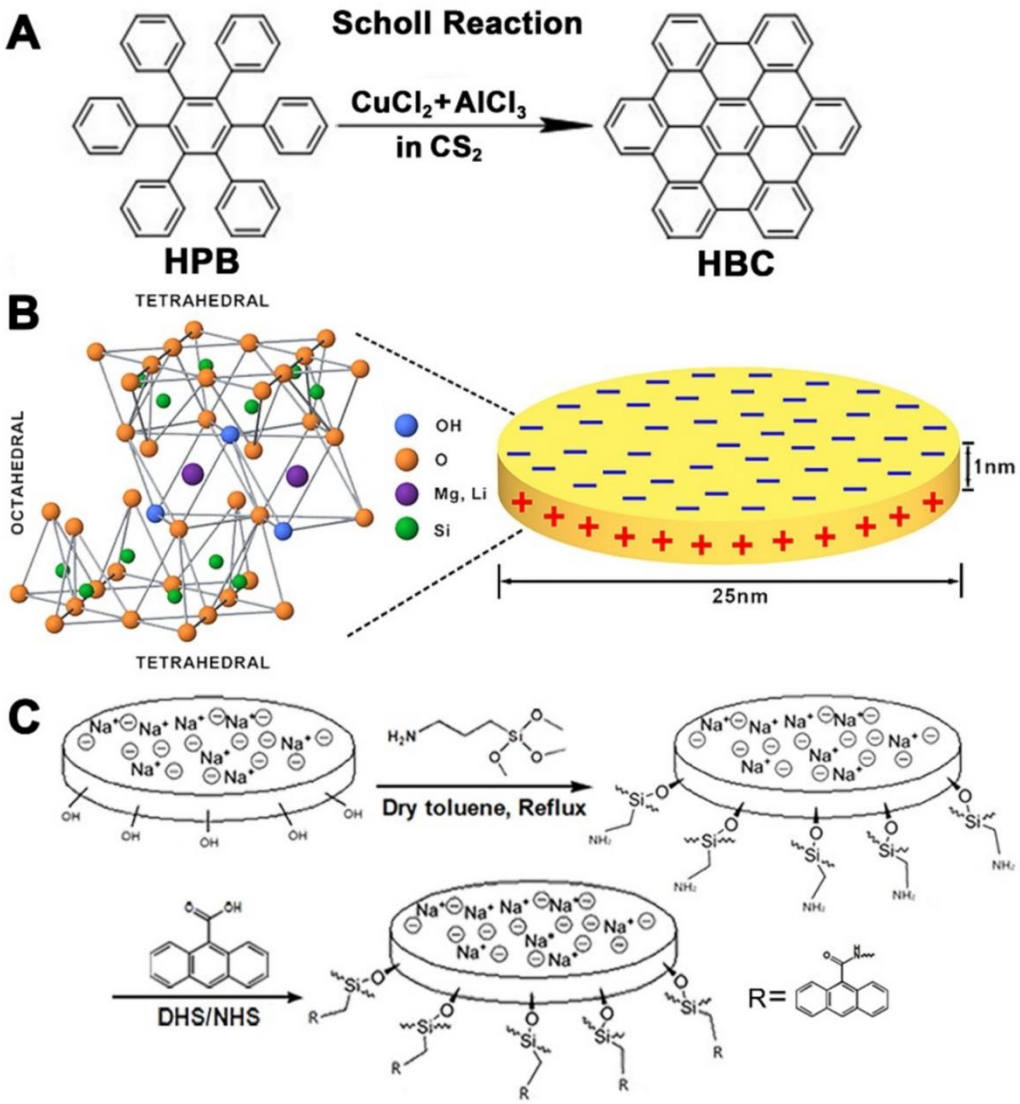

Figure S1. Schematic diagrams on synthetic route of HBC (A), chemical structure (B) and edge decoration of the rounded LAP nanoclay (C).

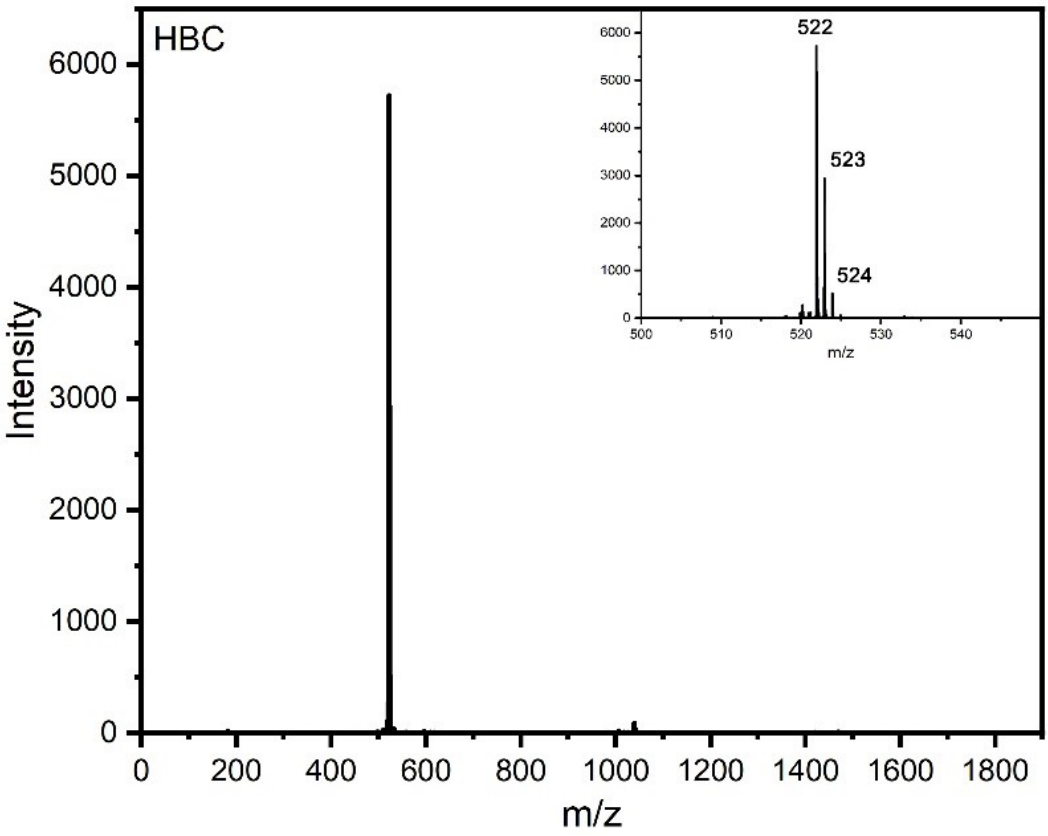

Figure S2. MALDI-TOF-MS spectrum of the synthesized HBC.

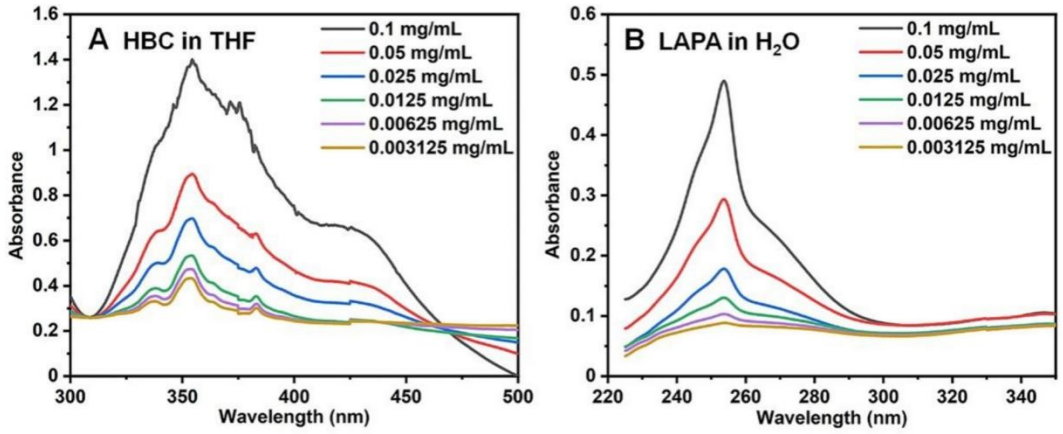

Figure S3. UV-Vis spectra of HBC (A; THF as solvent) and LAPA with different concentrations (B; deionized water as solvent).

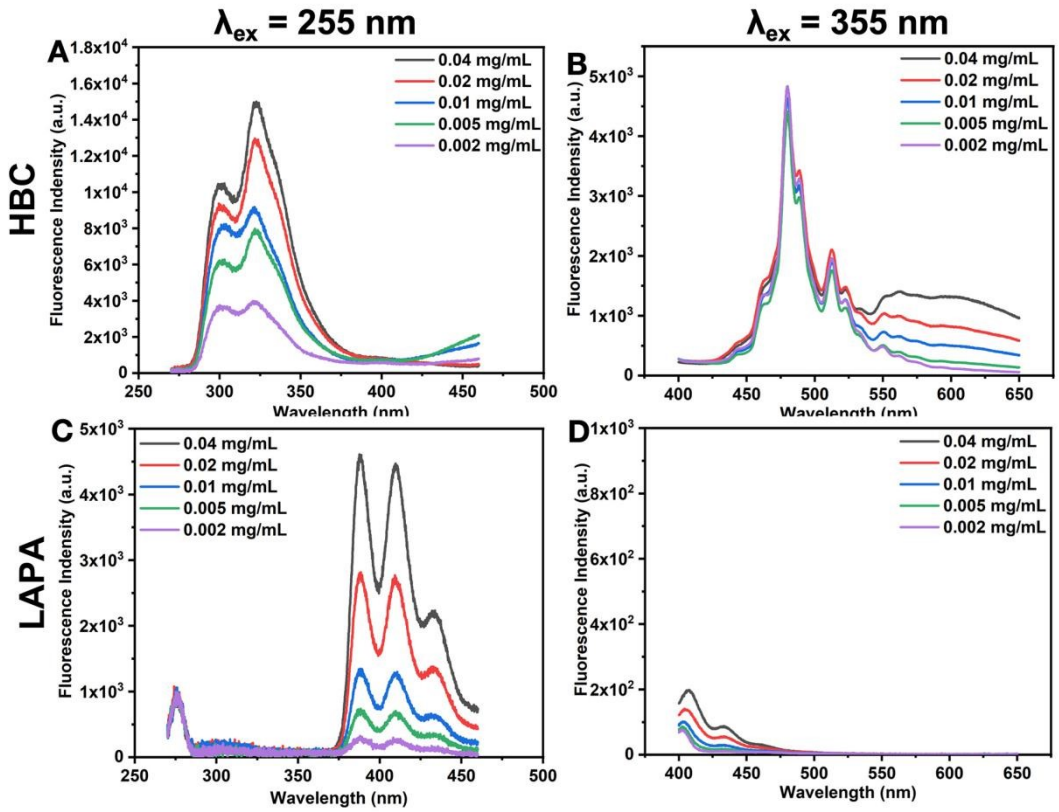

Figure S4. Two extracted fluorescence spectra with the two settled excitation wavelengths at different solute concentrations: HBC in THF, 255 (A) and 355 nm (B); LAPA in deionized water, 255 (C) and 355 nm (D).

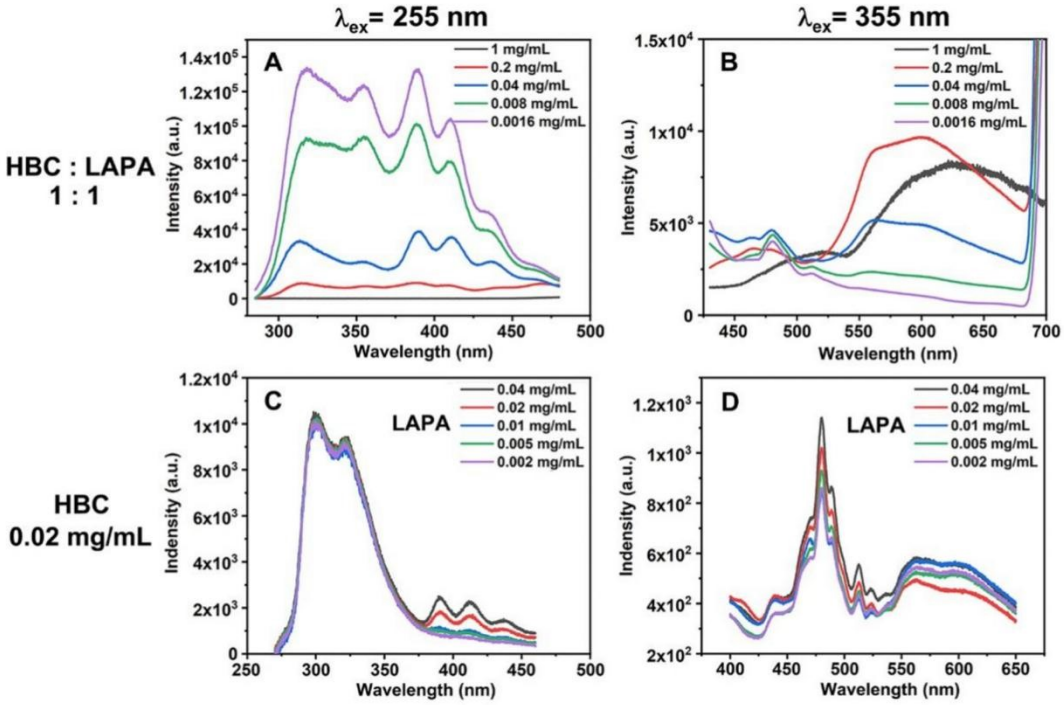

Figure S5. Fluorescence spectra of HBC@LAPA supramolecular nanoassemblies in the mixed solvent (volume ratio of THF to H_2O=1:1): upper line, different total solute concentrations with the same mass ratio of HBC and LAPA at 255 (A) and 355 nm (B); down line, different LAPA concentrations with the same HBC concentration of 0.02 mg/mL at 255 (C) and 355 nm (D).

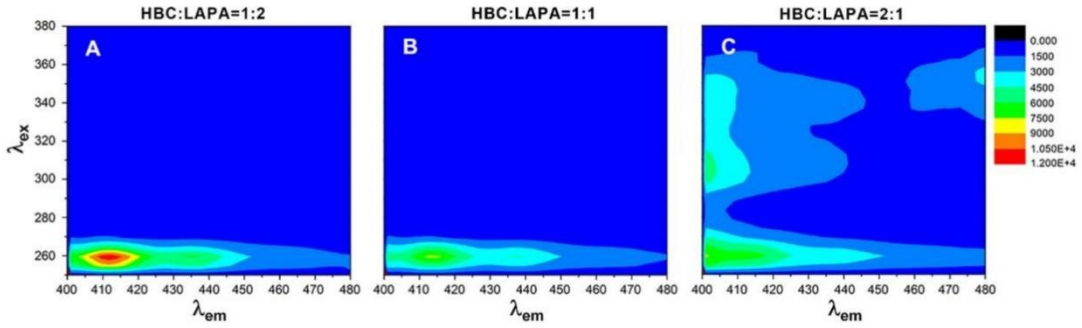

Figure S6. Three-dimension excitation emission matrix (3D-EEM) spectra of the resulting HBC@LAPA supramolecular assembly with different mass ratios in the mixed solvent (volume ratio of THF to H_2O=1:1).

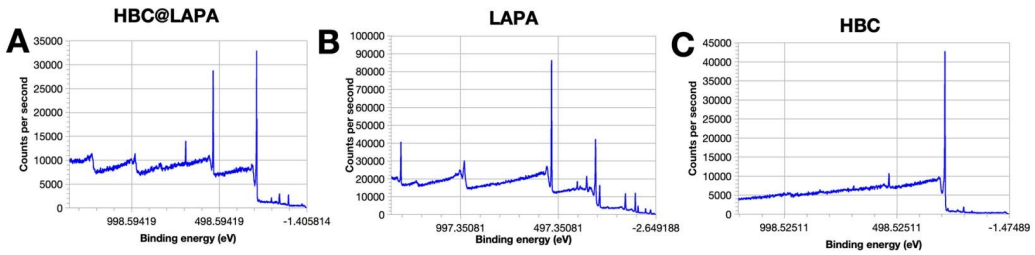

Figure S7. XPS spectra of HBC@LAPA (A), LAPA (B) and HBC (C).

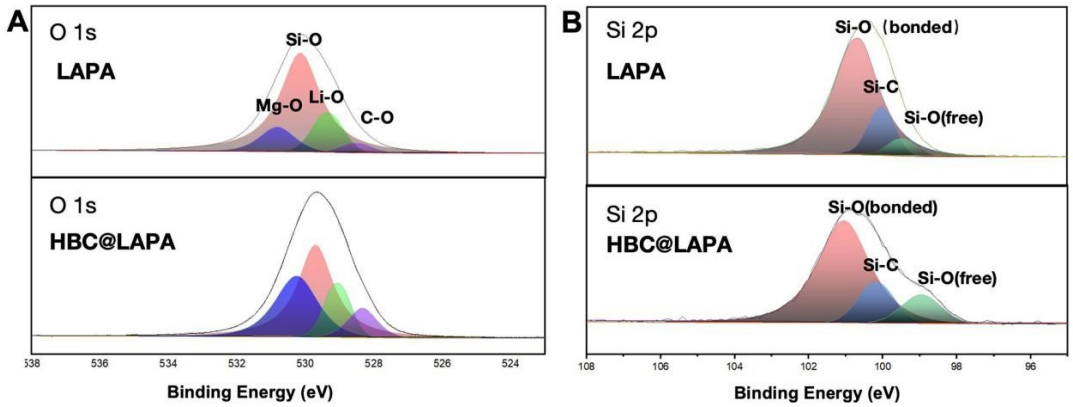

Figure S8 O 1s (A) and Si 2p characteristic peaks in the XPS spectra of the resulting LAPA nanoclays and HBC@LAPA nanoassemblies (B).

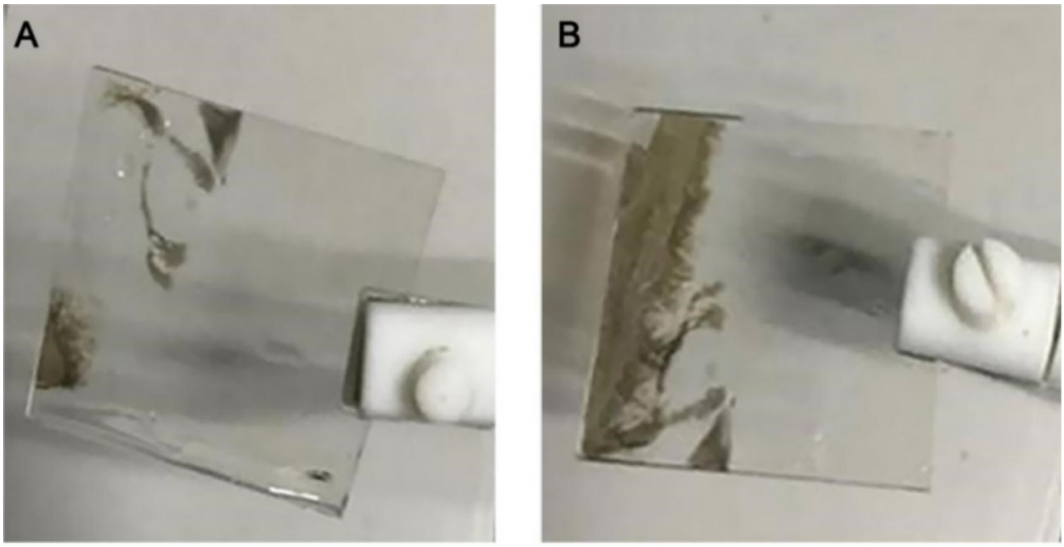

Figure S9. Real pictures of the ITO substrate as the cathode in the LC cell filling with HBC@LAPA supramolecular LC after the external direct current (DC) field was applied at 80 V for 1.5 (A) and 3 hours (B), respectively.

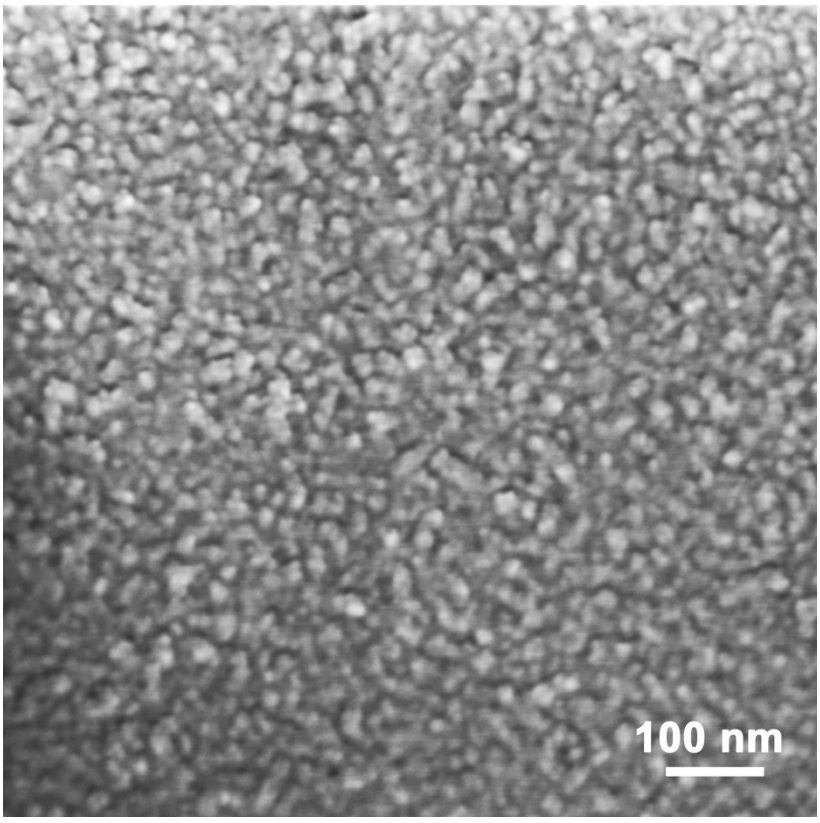

Figure S10. SEM image of the ITO substrate as the cathode in the planar ITO box filling with HBC@LAPA nanoassemblies after the external DC field was applied for 1 minute at 40 V.

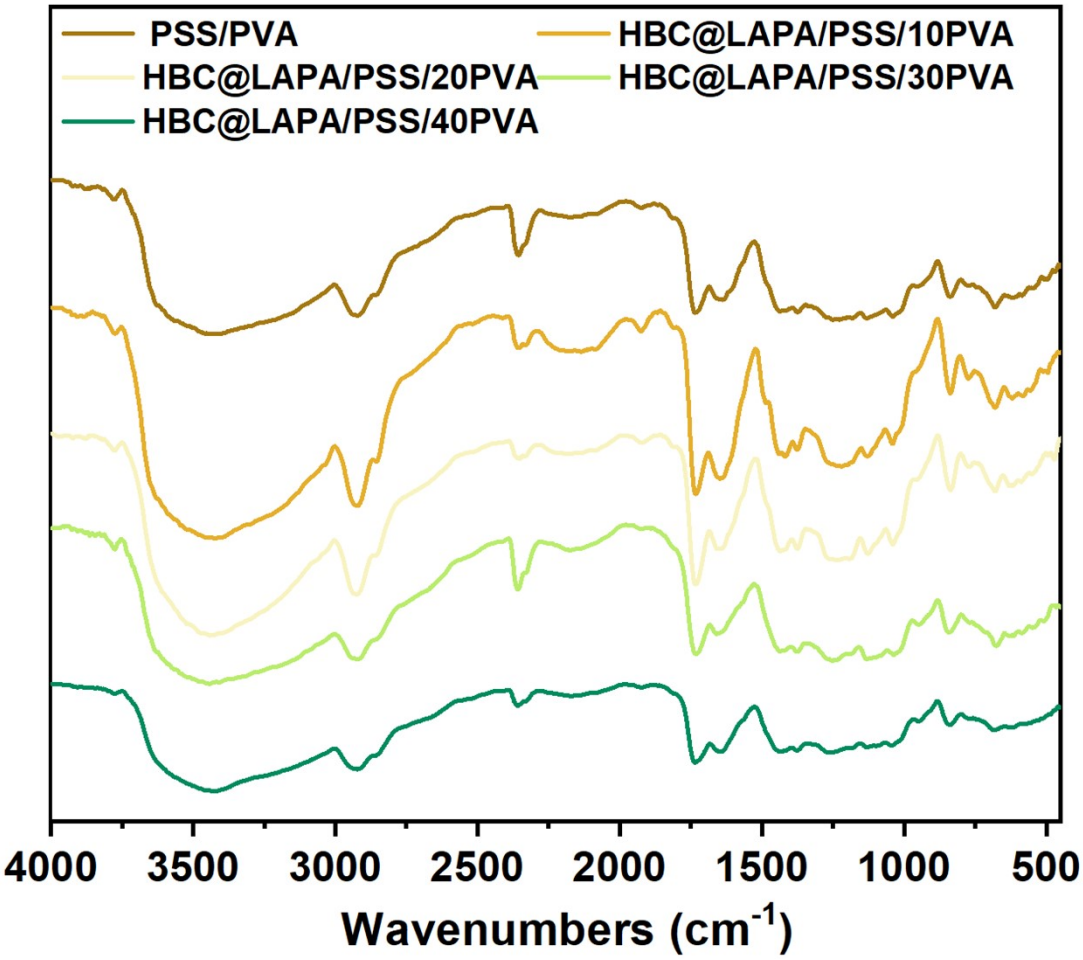

Figure S11. FT-IR spectra of HBC@LAPA/PSS/PVA membranes.

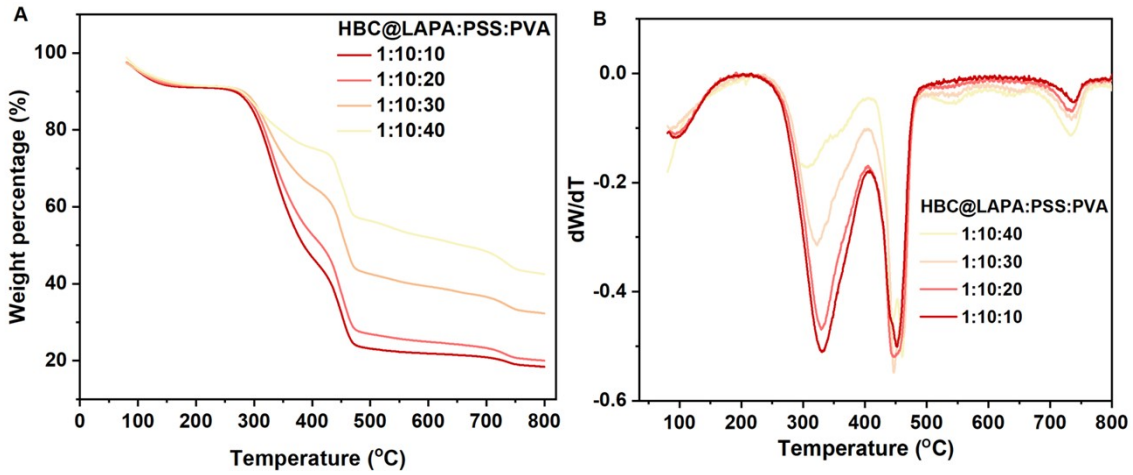

Figure S12. TGA (A) and DTG (B) curves of the HBC@LAPA/PSS/PVA gel under different PVA contents.

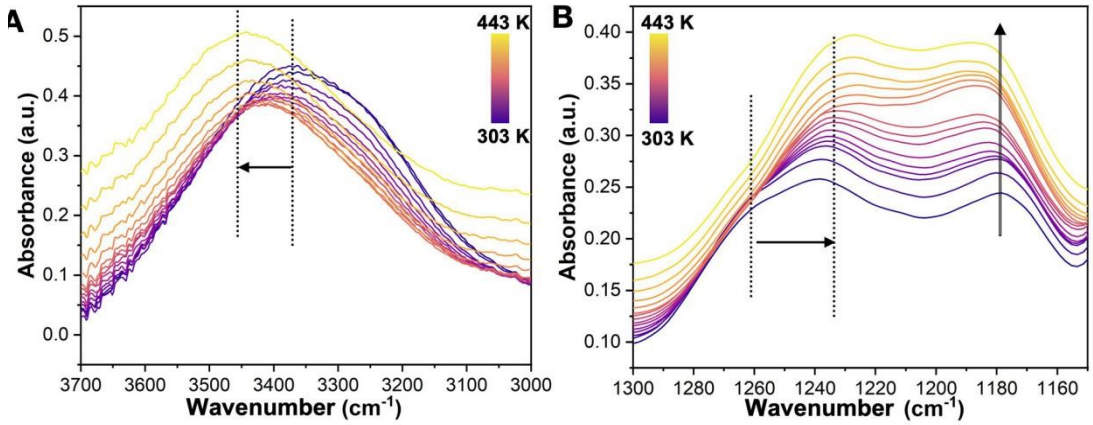

Figure S13. Variable temperature FT-IR spectra of the resulting HBC@LAPA/PSS/PVA membrane in the different wavenumber ranges of 3700- 3000 cm^{-1} (A), and 1300~1150 cm^{-1} (B).

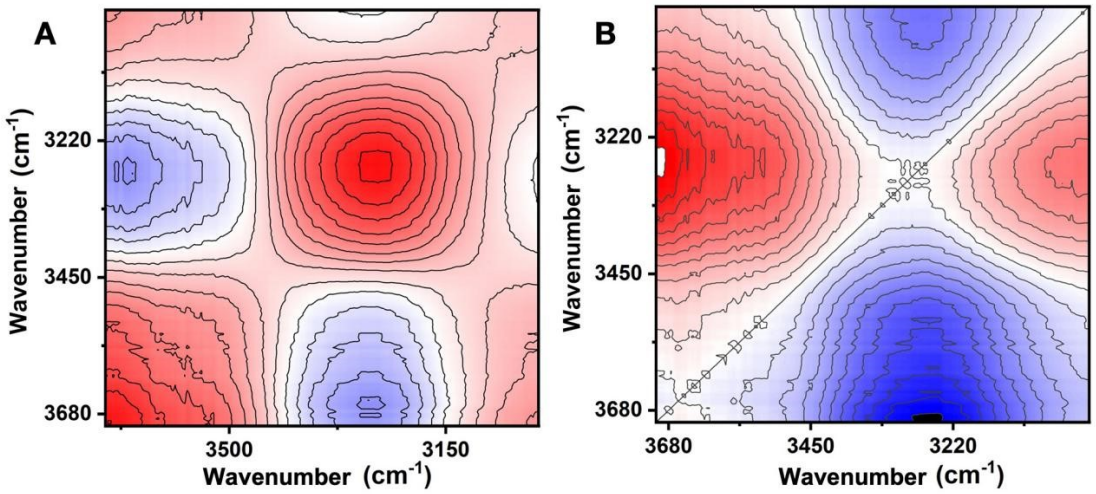

Figure S14. 2D correlation spectra of variable temperature FT-IR spectroscopy (2D COS FTIR) of the resulting HBC@LAPA/PSS/PVA membrane in the two different wavenumber ranges.

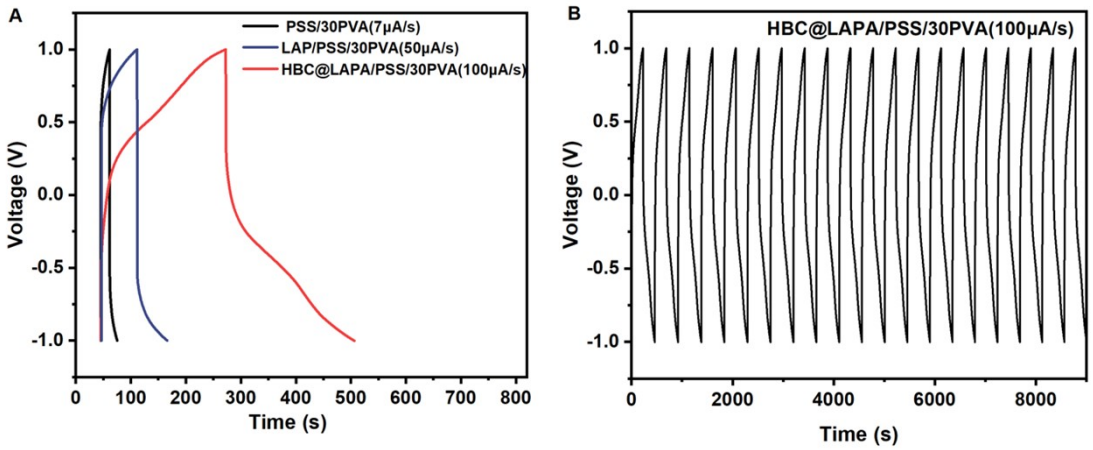

Figures S15 (A) Charge–discharge cycling performance of the PSS/PVA, LAP/ PSS/PVA and HBC@LAPA/PSS/PVA/ gel; (B) Charge–discharge cycles of HBC@LAPA/PSS/PVA/ gel.

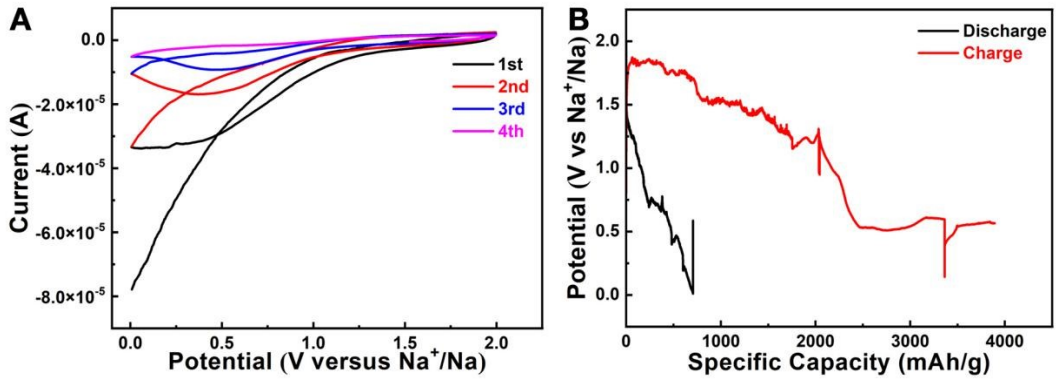

Figure S16. Test results of the HBC@LAPA/PSS/PVA membrane in the Li/S cell: cyclic voltammetry curves (A) and charge/discharge capacity (B).

Table S1 Comparison table on ionic conductivity of the gel polymer electrolytes.

Gel polymer electrolytes	σ (S/cm)	References
PEO+$NaCF_3SO_3$/SN	1.1×10^{-4}	S1
PEO+NaTf/TEGDME	2×10^{-4}	S2
PAN+NaI/EC/DMF	2.36×10^{-4}	S3
PVDF-HFP+EMITFSI-NaTFSI	2.5×10^{-4}	S4
PVDF+VA-PSVE-Na/P	1×10^{-4}	S5
PVDF-HFP+NaPTAB/PC	0.94×10^{-4}	S6
PVDF-HFP+NaPA/EC/DMC	0.91×10^{-4}	S7
Silica matrix+ NaTFSI/NMA	1.71×10^{-4}	S8
PSS/PVA+HBC@LAPA	2.81×10^{-4}	This work

References

S1. M. Patel.; K. G. Chandrappa.; A. J. Bhattacharyya.; *Solid State Ionics* **2010**, 181, 844.

S2. M. L. Lehmann.; G. Yang.; D. Gilmer.; K. S. Han.; E. C. Self.; R. E. Ruther.; S. R. Ge.; B. R. Li.; V. Murugesan.; A. P. Sokolov.; F. M. Delnick.; J. Nanda.; T. Saito.; *Energy Stor. Mater.* **2019**, 21, 85.

S3. N. K. Jyothi.; K. V. Kumar.; G. S. Sundari.; P. N. Murthy.; *Indian J. Phys.* **2016**, 90, 289

S4. D. T. Voa.; H. N. Doa.; T. T. Nguyena.; T. T. H. Nguyena.; V. M. Trana.; S. Okadac.; M. L. P. Le.; *Mater. Sci. Eng. B* **2019**, 241, 27.

S5. L. Y. Tian.; X. B. Huang.; X. Z. Tang.; *Eur. Polym. J.* **2004**, 40, 735

S6. L. Yang.; Y. Jiang.; X. Liang.; Y. Lei.; T. Yuan.; H. Lu.; Z. Liu.; Y. Cao.; J. Feng.; *ACS Appl. Energy Mater.* **2020**, 3, 10053

S7. Q. Y. Pan.; Z. Li.; W. C. Zhang.; D. L. Zeng.; Y. B. Sun.; H. S. Cheng.; *Solid State Ionics* **2017**, 300, 60.

S8. J. Mercken.; D. De Sloovere.; B. Joos.; D. Ghogare.; Y. Verhille.; S. Smeets.; E. Derveaux.; P. Adriaensens.; M. Van Bael.; A. Hardy, *ChemSusChem*, **2025**, 18: e202500427.